

Controlling turbulence in coupled map lattice systems using feedback techniques

P. Parmananda

Facultad de Ciencias, UAEM, Avenida Universidad 1001, Col. Chamilpa, Cuernavaca, Morelos, Mexico

M. Hildebrand and M. Eiswirth

Fritz-Haber-Institut der Max-Planck-Gesellschaft, Faradayweg 4-6, D-14195 Berlin, Germany

(Received 28 January 1997)

We report the suppression of spatiotemporal chaos observed in coupled map lattices. Suppression is achieved using different feedback techniques, most of which are applicable to actual experimental situations. Results from application of feedback control to a single chaotic element (single map) are presented to demonstrate similarities in the dynamical response of a single system and an extended system under the influence of external feedback. [S1063-651X(97)04607-2]

PACS number(s): 05.45.+b

I. INTRODUCTION

Suppression of the turbulent behavior observed in spatially extended nonlinear systems is of much practical interest. The growing interest in this field stems from the pioneering work done by Ott, Grebogi, and Yorke [1] in controlling chaos. Since then chaos has been controlled in various experimental systems [2–7] using different control strategies [8–10]. These efforts have been naturally extended to try to tame the complex dynamical behavior observed in distributed dynamical systems [11–14]. This control of spatiotemporal chaos leading up to the control of turbulence is much more complicated due to the existence of numerous unstable spatial modes, but, is more important too, because of its possible applications in plasma, laser devices, chemical, and biological systems where both spatial and temporal dependences need to be considered. In this paper, we propose using feedback techniques to suppress turbulent behavior observed in a one-dimensional coupled map lattice model with periodic boundary conditions as first considered by Kaneko [15,16] and described briefly in Sec. II. In Sec. III we implement two control strategies to stabilize a fixed point (corresponding to a period one solution) of a single logistic map. These control strategies (Secs. III A and III B) when appropriately implemented to the extended system (Sec. IV A) manifest striking similarity between the dynamical response of a single map and an extended system. Results from implementation of different global feedback techniques to the extended system are presented in Sec. IV B. Finally, in Sec. V we compare and contrast the various control strategies used and discuss the possibility of application to experimental situations.

II. COUPLED MAP LATTICE MODEL

The coupled map lattice model used here to manifest the efficiency of feedback techniques to suppress turbulent behavior has the following diffusive coupling [15,16]:

$$X_{n+1}(i) = (1 - \epsilon)f(X_n(i)) + \epsilon/2[f(X_n(i+1)) + f(X_n(i-1))], \quad (1)$$

where n is the discrete time step and i is a lattice point ($i = 1, 2, \dots, N = \text{system size}$). We restrict ourselves to choosing periodic boundary conditions. The mapping function $f(x)$ is chosen to be the logistic map described by

$$f(x) = (1 - ax^2). \quad (2)$$

The system parameter a is fixed such that the single map exhibits chaotic dynamics.

III. CONTROLLING CHAOS IN A SINGLE MAP USING SIMPLE FEEDBACK TECHNIQUES

In this section we apply two feedback techniques to control chaotic dynamics exhibited by a single logistic map [Eq. (2)]. Using the feedback control we were able to stabilize the fixed point of the map (corresponding to the unstable period one orbit).

A. Feedback: $\gamma(X_n - X_{n-1})$

This feedback is a discretized version of the derivative control technique [17] used to suppress oscillatory dynamics

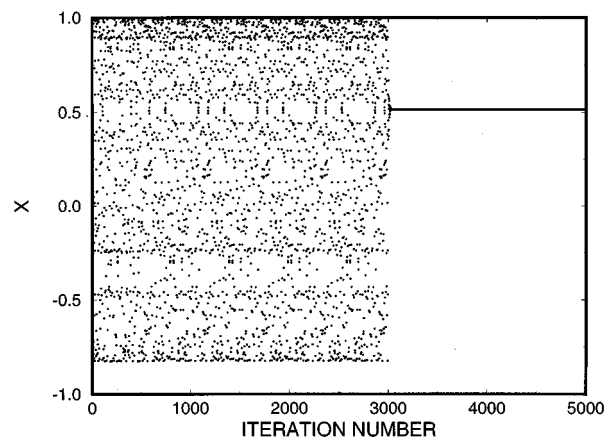


FIG. 1. Dynamical evolution of a single map without (<3000) control and under the influence of control (>3000) of the type as discussed in Sec. III A. The parameter a for the map is 1.81 and the control constant $\gamma = 0.95$.

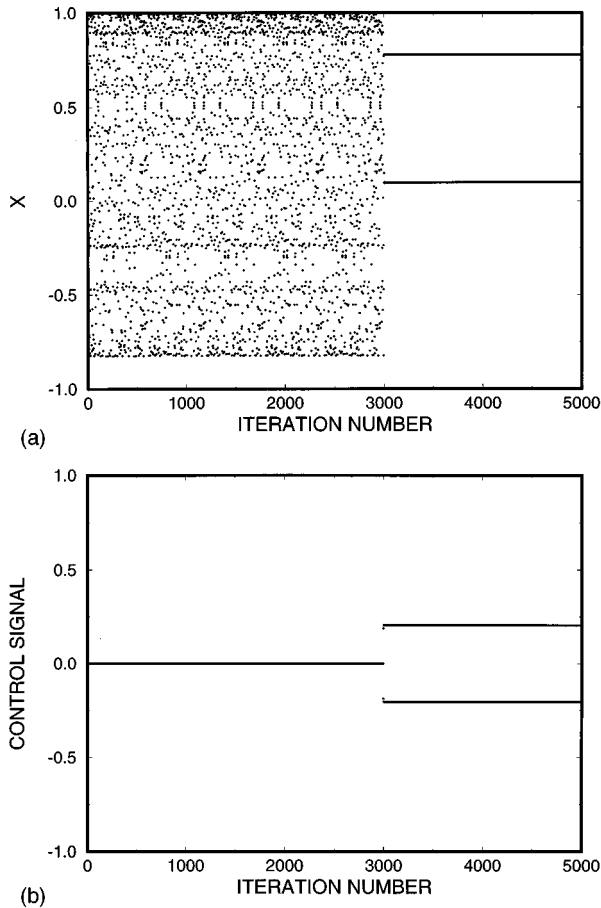


FIG. 2. Successful stabilization of the period-two fixed point of the map under the influence of the control of the type in Sec. III A. (a) Shows the dynamical evolution of the system. The value of the control constant is $\gamma=0.6$. Control is implemented subsequent to iteration number 3000. (b) Shows the nonvanishing control signal of the same period.

via stabilization of the previously unstable fixed points. Under the influence of the above mentioned control, the altered dynamics of the logistic map are represented by

$$X_{n+1} = (1 - aX_n^2) + \gamma(X_n - X_{n-1}). \quad (3)$$

Figure 1 shows the dynamical evolution of the system. Before iteration number 3000, the system evolves chaotically and subsequently converges to the stabilized fixed point under the influence of the control. Upon successful stabilization of the period-one orbit the control signal goes to zero as $X_n = X_{n-1}$.

As the value of γ was decreased we were able to stabilize the whole array of dynamical behavior of increasing complexity (period two, period four period eight, . . .). However, the control signal for such stabilizations did not go to zero. Figure 2(a) shows one such stabilization on the period-two orbit beyond iteration number 3000. The nonvanishing control signal is plotted in Fig. 2(b). This is not controlling chaos in the pure sense (as the control signal does not vanish upon successful stabilization) but more like altering dynamics via a nonvanishing feedback.

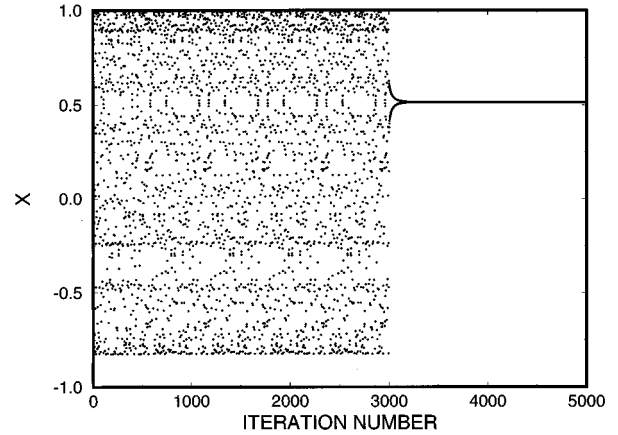


FIG. 3. Successful stabilization of the period-one fixed point of the map ($a=1.81$) using the control of the type in Sec. III B. The value of the control constant $\gamma=0.86$ was used to attain successful stabilization.

B. Feedback: $\gamma(X_n - X_F)$

The feedback strategy used here is an adaptation of the external force control technique [18] applied to temporal systems, such as

$$\frac{dx}{dt} = P(y, x) + F(t) \quad \frac{dy}{dt} = Q(y, x) \quad (4)$$

where y is the output variable and vector x describes the remaining variables. From the time series of $y(t)$, one can identify [19] the various periodic signals of different forms $y = y_i(t)$, $y_i(t + T_i) = y_i(t)$ corresponding to the different unstable periodic orbits. Here T_i is the period of the i th unstable orbit. $F(t)$ in Eq. (4) is the superimposed feedback described by

$$F(t) = \gamma[y_i(t) - y(t)]. \quad (5)$$

When applied to a single logistic map the above control strategy is expressed as

$$X_{n+1} = (1 - aX_n^2) + \gamma(X_n - X_F). \quad (6)$$

Figure 3 represents the dynamical evolution of the system without control (iteration < 3000) and with control (iteration > 3000). The control signal upon successful stabilization goes to zero as the dynamics converge onto the target period-one orbit (fixed point of the map X_F). Similar to the results discussed in the preceding subsection, by decreasing γ we were able to stabilize the entire array of dynamical behavior with a nonvanishing control signal.

IV. SUPPRESSION OF TURBULENCE IN A COUPLED MAP LATTICE SYSTEM

In this section we consider the extended system (100 coupled maps) with periodic boundary conditions studied extensively by Kaneko [15,16] and mentioned briefly in Sec. II. The coupled map system exhibits turbulent dynamics for the following parameter values ($a=1.81$ and $\epsilon=0.08$). The implemented control strategies are presented in different sub-

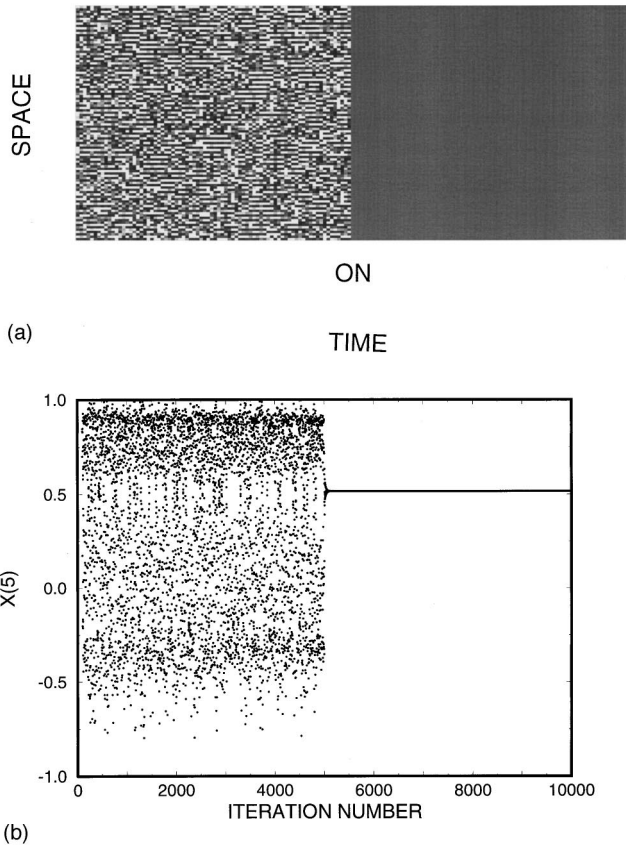


FIG. 4. Control of the turbulent behavior via stabilization of the homogeneous state for a 100 coupled logistic maps using the control as discussed in Sec. IV A 1. The system parameter is $a = 1.81$ and the coupling constant is $\epsilon = 0.08$. The value of the control constant $\gamma = 0.9$ achieves the desired stabilization. (a) Space-time portrait before and subsequent to (indicated by “ON”) implementation of the control signal. Every 64th step is plotted along the time axis. (b) Depicts the local time series of the fifth cell before and subsequent to the implementation of the control. The stabilization occurs on the previously unstable fixed point solution of the map.

sections depending on whether or not the local state of the system is required for their successful implementation. All the discussed feedback strategies are able to suppress the turbulent dynamics via stabilization of fixed point (homogeneous state) or periodic (clustered state) solutions.

A. Local feedback techniques

All the feedbacks considered in this subsection require information of the local state for successful suppression of the turbulent dynamics. Although the feedback is implemented locally, the feedback superimposed to the evolution equation is the difference between the local state and a global observable (local-global composite).

$$1. \text{ Feedback: } \gamma(X_n^i - 1/N \sum_{i=1}^N X_{n-1}^i)$$

The altered dynamics under the influence of the above feedback control is represented by

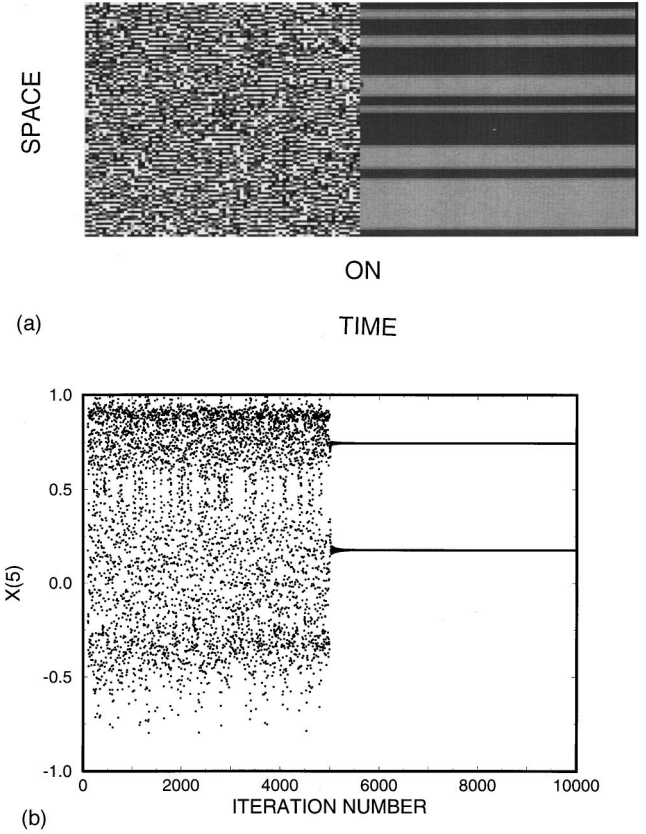


FIG. 5. Stabilization of the periodic clustered state for the coupled map lattice with the implementation of the control, as discussed in Sec. IV A 1. The system parameter is $a = 1.81$ and the coupling constant is $\epsilon = 0.08$. The value of the control constant used is $\gamma = 0.6$. The control signal in this case is nonvanishing. (a) Space-time portrait exhibiting the control on the clustered state subsequent (indicated by “ON”) to implementation of the feedback control. Every 64th step is plotted along the time axis. (b) The local time series of the fifth cell before and subsequent to the implementation of the control. Similar to Fig. 2(a), stabilization occurs on the period-two state.

$$X_{n+1}(i) = (1 - \epsilon)f(X_n(i)) + \epsilon/2[f(X_n(i+1)) + f(X_n(i-1))] + \gamma \left(X_n^i - \frac{1}{N} \sum_{i=1}^N X_{n-1}^i \right). \quad (7)$$

Using the control of the type in Eq. (7) we were able to stabilize both the homogeneous and/or the clustered state depending on the value of γ . Figure 4(a) shows the space-time plot where the control is initiated at the time step 5000 and the dynamics stabilize on the homogeneous state. Figure 4(b) shows the local time series for the fifth cell. It exhibits the stabilization of the system dynamics on the fixed point of the map ($X_F = 0.516$) (identical to Fig. 1). Also the control signal vanishes upon successful stabilization. Figure 5(a) shows the space-time plot for the control at a lower value of γ . In this case the control stabilizes a clustered state corresponding to a periodic solution. The local time series of the fifth cell shows a period-two oscillation subsequent to the application of the control similar to the one shown in Fig.

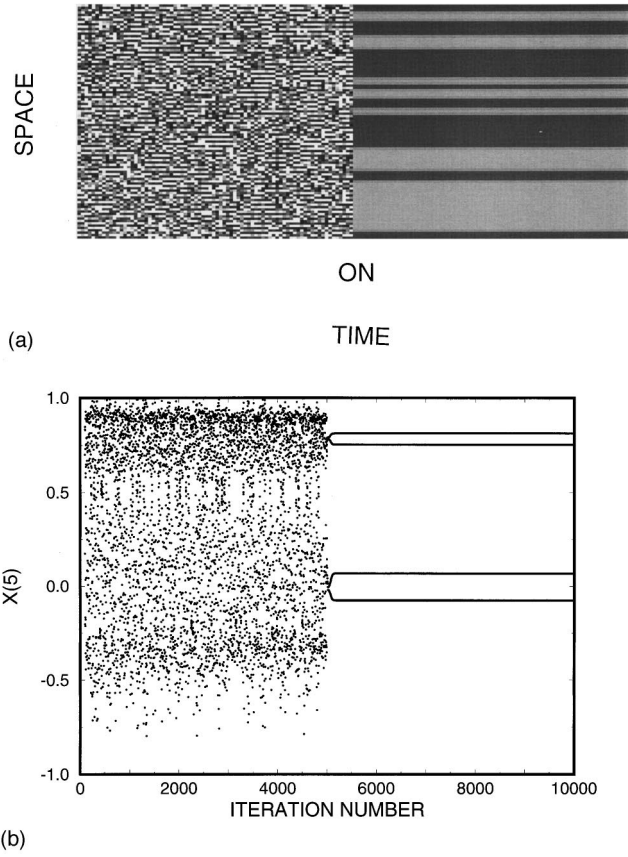


FIG. 6. Stabilization of the periodic clustered state for the coupled map lattice with the implementation of the control as discussed in Sec. IV A 2. The system parameter is $a=1.81$ and the coupling constant is $\epsilon=0.08$. The control constant $\gamma=0.4$ and the control signal is nonvanishing. (a) Space-time portrait exhibiting the control on the clustered state subsequent (indicated by “ON”) to implementation of the feedback control. Every 64th step is plotted along the time axis. (b) The local time series of the fifth cell before and subsequent to the implementation of the control. The stabilization occurs on the period-four state.

2(a). Also, the control signal for such a control is nonvanishing and exhibits a period-two oscillation similar to Fig. 2(b).

2. Feedback: $\gamma(X_n^i - X_F)$

The controlled dynamics under the influence of this feedback is represented by

$$X_{n+1}(i) = (1 - \epsilon)f(X_n(i)) + \epsilon/2[f(X_n(i+1)) + f(X_n(i-1))] + \gamma(X_n^i - X_F) \quad (8)$$

The control of Eq. (8) was also able to stabilize the homogeneous state. Moreover, as shown in the space-time plot of Fig. 6(a) suppression of turbulent dynamics was also achieved via stabilization of a clustered states with a nonvanishing control signal. The local time series for the fifth cell exhibiting a period-four oscillation is shown in Fig. 6(b). Also, the scenario of stabilizing structures (clusters) of higher complexity as γ decreases is observed, similar to the single map results for the similar feedback control (Sec. III B).

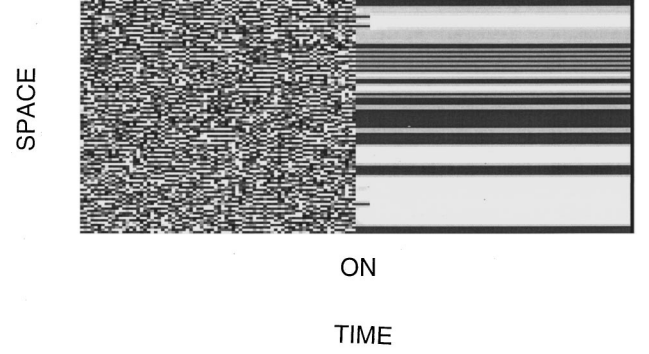


FIG. 7. Space-time portrait for a coupled lattice with the implementation (indicated by “ON”) of the control as discussed in Sec. IV B 1. The system parameter is $a=1.81$ and the coupling constant is $\epsilon=0.08$. Control constant $\gamma=0.45$ stabilizes periodic clustered state with a nonvanishing control signal. Every 64th step is plotted along the time axis.

B. Global feedback techniques

The obvious advantage of using global feedback techniques is the enhanced relevance to experimental situations. The feedbacks considered in this section involves superimposing a global observable (or difference between two global observables) to the dynamical equation.

1. Feedback: $-\gamma(1/N \sum_{i=1}^N X_{n-1}^i - 1/N \sum_{i=1}^N X_n^i)$

This control involves computing the difference in magnitude of successive global averages and feeding it back into the system. The system under the influence of the control is represented by

$$X_{n+1}(i) = (1 - \epsilon)f(X_n(i)) + \epsilon/2[f(X_n(i+1)) + f(X_n(i-1))] - \gamma \left(\frac{1}{N} \sum_{i=1}^N X_{n-1}^i - \frac{1}{N} \sum_{i=1}^N X_n^i \right). \quad (9)$$

A control of this type is plausible in an actual experimental system as the feedback required can be acquired from experiments. Using this control we were able to stabilize different clustered states with a nonvanishing control signal for different values of γ . Figure 7 shows the space-time plot for one such control exhibiting stabilization on a clustered (oscillatory yet periodic) state.

2. Feedback: $-\gamma(1/N \sum_{i=1}^N X_{n-1}^i - X_F)$

The motivation for trying this feedback are its possible applications to experimental situations. The results were similar to the one in the preceding subsection, namely, that suppression of the observed turbulent behavior is obtained via stabilization of the system dynamics on a clustered (oscillatory yet periodic) state. The altered dynamics under the influence of control are represented by

$$X_{n+1}(i) = (1 - \epsilon)f(X_n(i)) + \epsilon/2[f(X_n(i+1)) + f(X_n(i-1))] - \gamma \left(\frac{1}{N} \sum_{i=1}^N X_{n-1}^i - X_F \right). \quad (10)$$

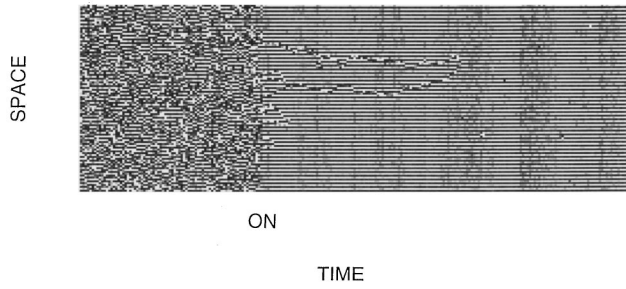


FIG. 8. Space-time portrait for a coupled lattice with the implementation of the control (indicated by “ON”) as discussed in Sec. IV B 2. The system parameter is $a = 1.81$ and the coupling constant is $\epsilon = 0.08$. Value of the control constant $\gamma = 0.35$ results in stabilization of the periodic clustered state with a nonvanishing control signal. Every 64th step is plotted along the time axis.

Figure 8 exhibits the eventual stabilization on the clustered state subsequent to implementation of the control. The system was integrated under the influence of control until successful suppression of the defect was achieved.

$$3. \text{ Feedback: } -\gamma \mathbf{1}/N \sum_{i=1}^N X_{n-1}^i$$

Global delayed feedback has been used to control turbulence in the complex Ginzburg-Landau equation [14]. In this subsection we implement a global feedback with delay to the coupled map lattice system exhibiting chaotic behavior. The dynamics under the influence of the control is represented by

$$X_{n+1}(i) = (1 - \epsilon)f(X_n(i)) + \epsilon/2[f(X_n(i+1)) + f(X_n(i-1))] - \gamma \frac{1}{N} \sum_{i=1}^N X_{n-1}^i. \quad (11)$$

Figure 9 shows the results of implementation of the global feedback control. Control is attained on a homogeneous state, however the control signal remains a nonvanishing entity. By varying the value of γ we were able to stabilize a

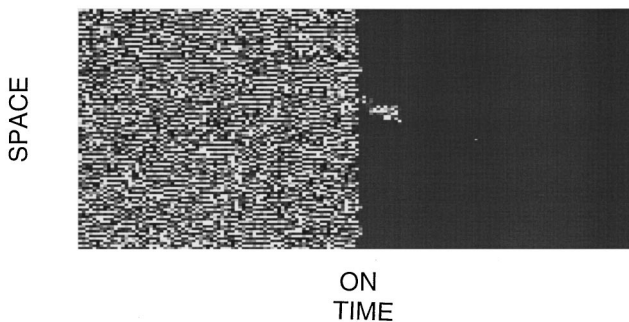


FIG. 9. Space-time portrait for a coupled lattice with the implementation of the global feedback control (indicated by “ON”) as discussed in Sec. IV B 3. The system parameter is $a = 1.81$ and the coupling constant is $\epsilon = 0.08$. The value of the control constant $\gamma = 0.34$ results in stabilization of the homogeneous state with a nonvanishing control signal. Every 64th step is plotted along the time axis.

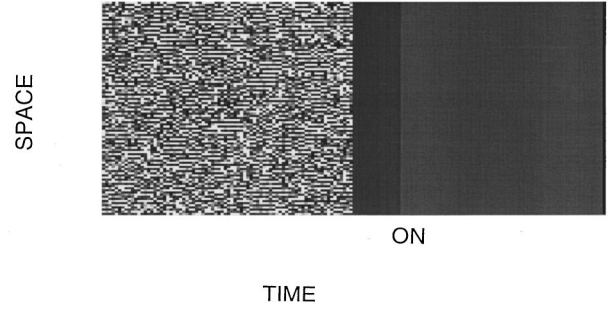


FIG. 10. Space-time portrait for a coupled lattice with the implementation (indicated by “ON”) of the feedback control as discussed in Sec. IV B 4. The system parameter a is reduced to $a = 0.5$ for 1000 iterations (simulating a spike) to attain the initial homogeneous state. Subsequently the system parameter is reset to $a = 1.81$ and the control of Sec. IV B 4 is implemented with $\gamma = 0.7$ resulting in stabilization on the homogeneous state with a vanishing control signal. Every 64th step is plotted along the time axis.

wide array of nonturbulent oscillatory dynamical behavior (clusters). It should be possible to apply this global feedback control to actual systems.

$$4. \text{ Feedback: } -\gamma(\mathbf{1}/N \sum_{i=1}^N X_{n-1}^i - \mathbf{1}/N \sum_{i=1}^N X_n^i)$$

This is the identical feedback discussed in Sec. IV B 1, but it is applied to the system stabilized at the homogeneous state attained using a judiciously chosen parameter spike. The motivation for this is the following: It is possible to bring the system from the turbulent state to a homogeneous (nonsimilar to the target homogeneous state on which control is desired) state momentarily via a parameter manipulation (kind of resetting the system). Now once the system is at the temporary homogeneous state a control of the type such as above is applied to try to constrain the system dynamics on the target homogeneous state (corresponding to the previously unstable fixed point of the map). Figure 10 shows the results of such a two-step control exhibiting the system stabilization on a homogeneous steady state. Control of this sort is possible in an actual experiment provided that the system can be resetted via a judicious parameter spike.

V. CONCLUSIONS

In this article we have demonstrated successful suppression of turbulent behavior observed under appropriate parameter conditions in the one-dimensional coupled map lattice system. The stabilized system corresponded to the homogeneous state and/or the clustered state depending on the type of feedback used and/or the value of γ chosen. The remarkable analogy between the dynamical behavior under the influence of the control between a single map (Secs. III A and III B) and a lattice of coupled maps (Secs. IV A 1 and IV A 2) is described. The feedback control described in Secs. IV A 1 and IV A 2 requires information about the local state of the system for successful implementation, however it does not necessary imply that they are not applicable to experimental situations. The controlling feedback in both these strategies is proportional to the difference between the local

state and a global variable. Therefore, the correctional feedback superimposed on a site is related to the local dynamics at that site. It is possible to envisage a setup (for example, using optical illumination as the control parameter) where the response on different sites of an extended system is a function of the local state of individual sites. Only partial suppression of turbulent dynamics could be achieved if the control was applied to a subset of the lattice because of the inherent absolute instability of the model system. However, suppression of turbulent dynamics via implementation of control to selected sites is possible [12] if the underlying system exhibits convective instability. The following four

control strategies (Secs. IV B 1–IV B 4) rely on feedbacks involving global observables and are more generally applicable to experimental situations.

ACKNOWLEDGMENTS

We have benefited greatly from discussions with Professor Gehard Ertl at the Fritz-Haber Institute. One of us (P.P.) acknowledges financial support from CONACyT under Project Ref. No. 4873 and from the Alexander Von Humboldt Foundation.

-
- [1] E. Ott, C. Grebogi, and J. A. Yorke, *Phys. Rev. Lett.* **64**, 1196 (1990).
 - [2] W. L. Ditto, S. N. Rausero, and M. L. Spano, *Phys. Rev. Lett.* **65**, 3211 (1990).
 - [3] E. R. Hunt, *Phys. Rev. Lett.* **67**, 1953 (1991).
 - [4] R. Roy, T. Murphy, Jr., T. D. Maier, Z. Gills, and E. R. Hunt, *Phys. Rev. Lett.* **68**, 1259 (1992).
 - [5] A. Garfinkel, M. L. Spano, W. L. Ditto, and J. N. Weiss, *Science* **257**, 1230 (1992).
 - [6] V. Petrov, V. Gáspár, J. Masere, and K. Showalter, *Nature (London)* **361**, 240 (1993).
 - [7] P. Parmananda, P. Sherard, R. W. Rollins, and H. D. Dewald, *Phys. Rev. E* **47**, R3003 (1993).
 - [8] B. Peng, V. Petrov, and K. Showalter, *J. Phys. Chem.* **95**, 4957 (1991).
 - [9] B. Peng, V. Petrov, and K. Showalter, *Physica A* **188**, 210 (1992).
 - [10] R. W. Rollins, P. Parmananda, and P. Sherard, *Phys. Rev. E* **47**, R780 (1993).
 - [11] Hu Gang and Qu Zhilin, *Phys. Rev. Lett.* **72**, 68 (1994).
 - [12] Ditzia Auerbach, *Phys. Rev. Lett.* **72**, 1184 (1994).
 - [13] Igor Aranson, Herbert Levine, and Lev Tsimring, *Phys. Rev. Lett.* **72**, 2561 (1994).
 - [14] D. Battogtokh and A. Mikhailov, *Physica D* **90**, 84 (1996).
 - [15] Kunihiko Kaneko, *Physica D* **34**, 1 (1989).
 - [16] Kunihiko Kaneko, *Physica D* **37**, 60 (1989).
 - [17] S. Biewalski, M. Bouazaoui, D. Derozier, and P. Glorieux, *Phys. Rev. A* **47**, 3276 (1993).
 - [18] K. Pyragas, *Phys. Lett. A* **170**, 421 (1992).
 - [19] D. P. Lathrop and E. J. Kostelich, *Phys. Rev. A* **40**, 4028 (1989).